Dynamic radiography using a carbon-nanotube-based field-emission x-ray source

Y. Cheng and J. Zhang
Department of Physics and Astronomy, University of North Carolina, Chapel Hill, North Carolina 27599

Y. Z. Lee
Department of Biomedical Engineering, University of North Carolina, Chapel Hill, North Carolina 27599

B. Gao
Xintek, Inc., 308 W Rosemary St., Chapel Hill, North Carolina 27516

S. Dike
Curriculum in Applied and Materials Sciences, University of North Carolina, Chapel Hill, North Carolina 27599

W. Lin
Department of Radiology, School of Medicine, University of North Carolina, Chapel Hill, North Carolina 27599

J. P. Lu and O. Zhou[a)]
Department of Physics and Astronomy, University of North Carolina, Chapel Hill, North Carolina 27599 and Curriculum in Applied and Materials Sciences, University of North Carolina, Chapel Hill, North Carolina 27599

(Received 22 March 2004; accepted 24 June 2004; published 20 September 2004)

We report a dynamic radiography system with a carbon nanotube based field-emission microfocus x-ray source. The system can readily generate x-ray radiation with continuous variation of temporal resolution as short as nanoseconds. Its potential applications for dynamic x-ray imaging are demonstrated. The performance characteristics of this compact and versatile system are promising for noninvasive imaging in biomedical research and industrial inspection. © *2004 American Institute of Physics.* [DOI: 10.1063/1.1791313]

I. INTRODUCTION

Time-resolved x-ray radiography is a noninvasive imaging technique that provides dynamic information of an object's internal structure which is vital for fields such as medical imaging, materials science, and nondestructive evaluation.[1,2] The principle of this technique is simple: Either the radiation or/and the data collection time needs to be sufficiently shorter than the time scale of the phenomena under investigation. Conventional thermionic x-ray tubes which are the most common sources of x-ray radiation have limited temporal resolution. Grid-controlled tubes which are among the fastest thermionic x-ray tubes can produce 0.1–10 millisecond (ms)-width x-ray radiation. In addition to limited temporal resolution, thermally emitted electrons have random spatial distribution which is difficult to focus. The focal spots of thermionic tubes usually have a bimodal intensity distribution perpendicular to the axis of the tube,[3] which results in a undesirable modulation transfer function and limits the spatial resolution.[4]

X-ray sources with field-emission[5] cathodes in principle have significant advantages over the current thermionic systems especially in temporal and spatial resolution which are important for biomedical imaging, inspection of microelectronics, and dynamic studies.[6] With an instantaneous response time, x-ray radiation with programmable wave form and high temporal resolution can be generated using the field emission cathode, which is desired for time-resolved x-ray radiography. Field emitted electrons intrinsically have low divergence and in principle are easy to focus, which can lead to high spatial resolution. Although field emission x-ray sources have been experimented on and tested for clinical use in the past,[7,8] these early experimental systems suffered from high extraction field and short lifetime due to the limitations of the field emitters. Microfabricated tips and diamond-based emitters have been proposed as the cold-cathodes for x-ray tubes but have failed to show high enough emission current and environmental stability to be viable for actual devices.[9,10] Carbon nanotubes (CNTs)[11,12] are shown to have a low threshold field for emission and high current capability.[13–15] CNT based cold-cathode electronic devices are being actively investigated.[16] Preliminary results have demonstrated the possibility of generating x-ray radiation using CNT and CNT-like field emitters.[17–20] Here we report the development of a CNT based microfocus x-ray tube and an imaging system for dynamic radiography. The system can readily generate x-ray radiation with continuous variation of temporal resolution up to *nanoseconds*. By synchronizing

a)Electronic mail: zhou@physics.unc.edu

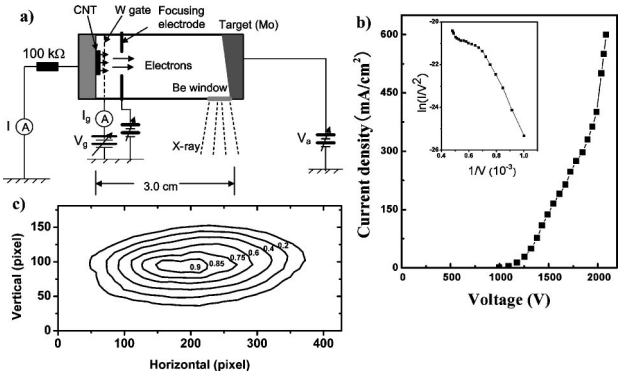

FIG. 1. (a) Schematic drawing of the CNT based microfocus x-ray tube. (b) Electron emission current (vs) applied voltage obtained from a 1 mm^2 CNT cathode. (c) Contour plot of the focal spot intensity distribution of the CNT-based x-ray tube.

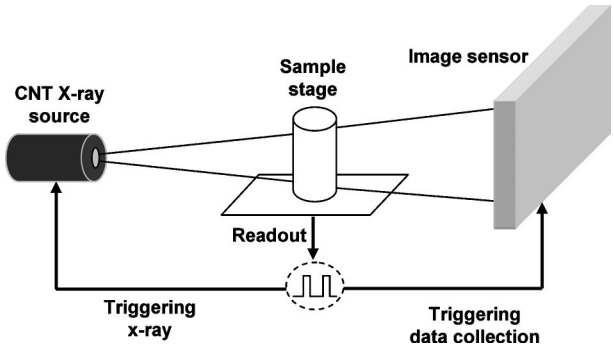

FIG. 2. Dynamic x-ray radiography system. For gated studies, data collection can be triggered by either the readout from a photosensor that monitors the location of the object or a pulse derived from the ventilator used in animal imaging.

x-ray exposure, data collection, and signals from the object such as the respiration rate of a live rat, the system enables triggered and gated imaging to obtain dynamic information at reduced x-ray dose.

II. CNT BASED MICROFOCUS X-RAY TUBE

The schematic of the micro-focus x-ray tube is shown in Fig. 1(a). It consists of a CNT field emission cathode, a focusing electrode, a gate electrode, and a Mo target housed in a vacuum chamber with a Be window. The tube current I_a (the emission current bombarding on the anode) is controlled by the voltage between the gate and cathode (V_g) while the x-ray photon energy is set by the acceleration voltage between the target and the cathode (V_a). In the current design a single focusing electrode was used. The design of the gate structure and the focusing electrode was aided by electromagnetic simulations of the electron optics using a commercial software. The focal-spot size was controlled by the potential of the focusing electrode.

The key performance characteristics of an x-ray source include flux, resolution, and stability. Significant efforts have been put into the selection of the CNT structure, the control of the CNT film morphology, and the design of the extraction and focusing electrode to ensure high emission current density, high transmission rate, and long-term stability. The electron source used for this study has a 1 mm-diameter cathode with randomly oriented CNTs. A peak emission current up to 6 mA (>760 mA/cm^2 density) was obtained at a gate electric field of ~ 15 V/μm ($V_g = 2060$ V) under pulsed mode [Fig. 1(b)]. The emission current was stable with $<1\%$ fluctuation up to the highest anode voltage used in this study ($V_a = 60$ kV). The focal spot size of the x-ray source which determines the spatial resolution was also evaluated according to a standard procedure.[21] A tungsten wire of 1 mm diameter was imaged using a relatively high geometric magnification. From the geometric unsharpness of the edge on the resulting image, the effective focal spot size of the CNT-based x-ray tube was estimated to be less than 150 μm(W) $\times 30$ μm(H). The intensity distribution of the focal spot obtained from a pinhole measurement shows the desired Gaussian distribution [Fig. 1(c)], not the double-peaked distribution commonly found on thermionic x-ray tubes. This favorable intensity distribution can provide better spatial resolution than either uniform or bimodal intensity distributions.[22]

III. DYNAMIC RADIOGRAPHY SYSTEM

The dynamic radiography system as illustrated in Fig. 2 comprises the CNT x-ray source, a sample stage, and a two-dimensiional digital x-ray image sensor (Hamamatsu C7921) measuring the transmitted x-ray intensity. The sensor contains a CsI scintillator plate, a 1056×1056 photodiode array with a total field of view of 52.8×52.8 mm. The available pixel size is 50 μm and the video output is a 12 bit digital signal with a bandwidth of 6.25 MHz. When running in 4×4 binning mode, it is capable of delivering a frame rate up to 16 frames per second (fps). In external trigger mode, the sensor is designed to read video data out at the rising edge of an external trigger signal, whose frequency then determines the frame speed. The x-ray pulses are turned on after finishing the readout of the previous frame and before the arrival of the next trigger signal. The readout of a frame takes 62 ms in the external trigger mode. The x-ray radiations during the readout time are not desired, so a delay between the rising edge of the trigger signal and that of the x-ray pulse was programmed to solve the problem. Thus, all unnecessary radiation exposures can be eliminated.

The image sensor is connected to a personal computer via an image acquisition board (NIPCI-1422). This board can capture up to 16 bits wide data at clock speeds up to 40 MHz. It has 16 MB onboard memory, which gives the flexibility to buffer images on the board before transferring them to the hard disk. The acquired image can also be buffered on the system memory, which has a relatively large capacity −512 MB. The one used for this study is compatible with the RS-422 video signal outputted by the image sensor.

The x-ray tube current that determines the x-ray flux is programmed by a digital pulse generator (Model: DEI PDG-2510) connected to the gate electrode (V_g). The pulse generator has an output for its synchronization signal T0, which marks the beginning of each timing cycle. This gives us the opportunity to trigger the image sensor by the T0 signal of the x-ray source. By synchronizing the timing cycle of x-ray generation with that of image acquisition, equilong x-ray il-

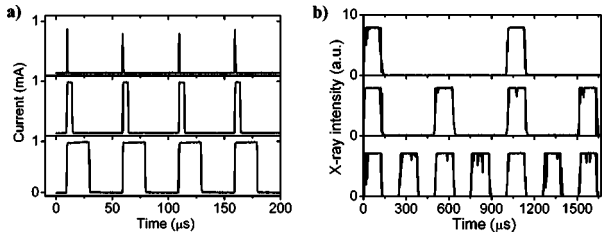

FIG. 3. (a) X-ray tube current with variable pulse width down to 0.5 μs at a constant repetition rate 20 kHz. (b) X-ray pulses of variable repetition rate at a constant width 150 μs obtained from a Si-PIN diode detector.

lumination time across every frame is guaranteed. For gated imaging, the digital pulse generator can be triggered by either a positioning signal from a moving object or a physiological pulse derived from a live animal. The pulse width and repetition rate of the x-ray radiation can be easily varied by programming the digital pulse generator at a fixed anode voltage (V_a), as shown in Fig. 3. There is a well-defined one-to-one correlation between the gate voltage and the x-ray tube current without delay. The rising and falling times of the 1-μs-width x-ray pulses were less than 0.1 μs. At present the shortest pulse generated was 50 ns which was limited by the capability of the digital pulse generator used in this study.

IV. IMAGING EVALUATION

The ability to program the emission current at rapid speed enabled dynamic x-ray imaging at a rate not achieved by thermionic x-ray sources. Figure 4 shows the x-ray images of a computer cooling fan rotating at ~1000 RPM taken under two different conditions. Image (a) was collected with 16 frames-per-seconds (fps) detector speed and continuous x-ray exposure which mimics the typical imaging condition of a conventional imaging system. The individual blades were not resolved, as expected. Images (b) and (c) were taken using the x-ray repetition rate $f=14$ Hz with a *single* millisecond-long x-ray pulse. The blades are still blurred with a 5 ms x-ray exposure in (b). Because the displacements of the blades within the 1 ms x-ray exposure time is

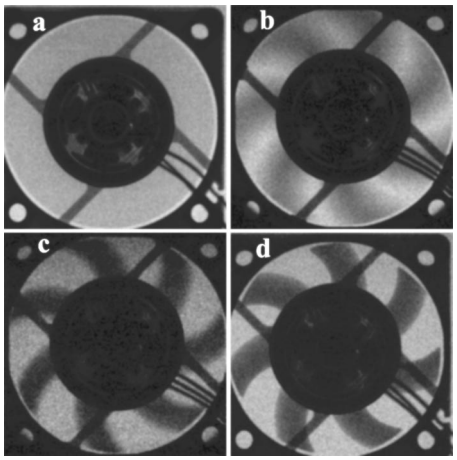

FIG. 4. Dynamic x-ray images of a fan (5 cm×5 cm) rotating at 1000 RPM taken using 16 fps detector speed (a) and x-ray pulse-widths of 5 ms (b) and 1 ms (c). For comparison, a static image of the fan is also shown (d).

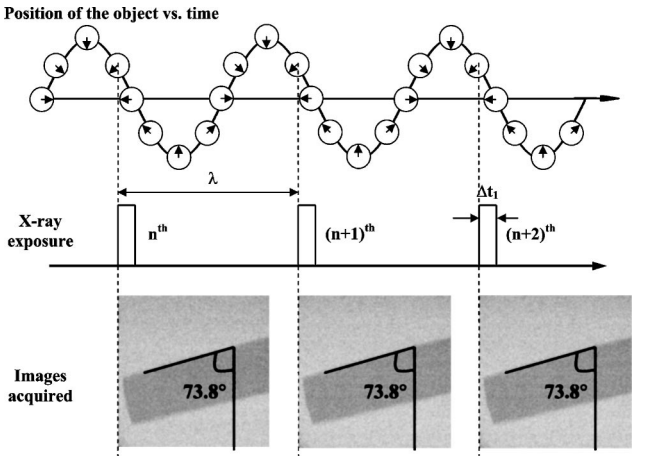

FIG. 5. Timing diagram of the imaging system and triggered images of a motor blade (9 cm×1 cm) rotating at about 100 RPM. The images were taken from three consecutive cycles using 2 ms x-ray pulse at 14 Hz. The images are identical.

negligible, the individual blades were clearly resolved in (c). A static image of the fan is also shown in (d) for comparison. Consecutive frames of 1 ms exposure can be acquired at the frame speed of the detector and compiled to an x-ray movie afterwards. Unblurred motion of the fan can be clearly resolved from the movie. The sharpness of the image increases with decreasing pulse width. By estimating the width of the blurred region and dividing it by the x-ray exposure time, the line speed of the moving object was obtained which agreed with the known value.

Gating provides position-specific structural information that is particularly important for advanced imaging modalities such as dynamic CT imaging of live objects.[23] It was readily accomplished in the present system. A single-blade fan rotating at 100 RPM was used as the phantom and a photogate was used to trigger x-ray exposure and data collection when the blade reached a predetermined position during rotation. A series of images from consecutive rotation cycles, one per cycle, were taken using 2-ms pulse-width, 14 fps detector speed, and 1 x-ray pulse per image. Figure 5 shows three frames of the blade from 3 consecutive rotation cycles. The images are essentially identical. Twenty images of the rotating blade obtained from 20 consecutive rotation cycles were summed to result in an image with signal-to-noise ratio increased from 2.6 to 12.5, which can be further increased to 15.3 when summing 30 frames of the same phase.

To further demonstrate the potential of the present system for biomedical imaging, prospectively respiration-triggered angiography studies were carried out on a live rat (Fig. 6). To distinguish a blood vessel from the surrounding tissues a contrast media (Omnipaque™) was injected into a vein connected to the heart of the rat. The respiration rate of the rat is controlled at 74/min via a respirator. A prospective trigger is derived from the respirator which is synchronized to the respiration rate of the rat. X-ray pulses of milliseconds duration are produced with a fixed delay after the trigger. In order to freeze the motion of the lungs of the rat, a single frame at the same position was acquired during each respi-

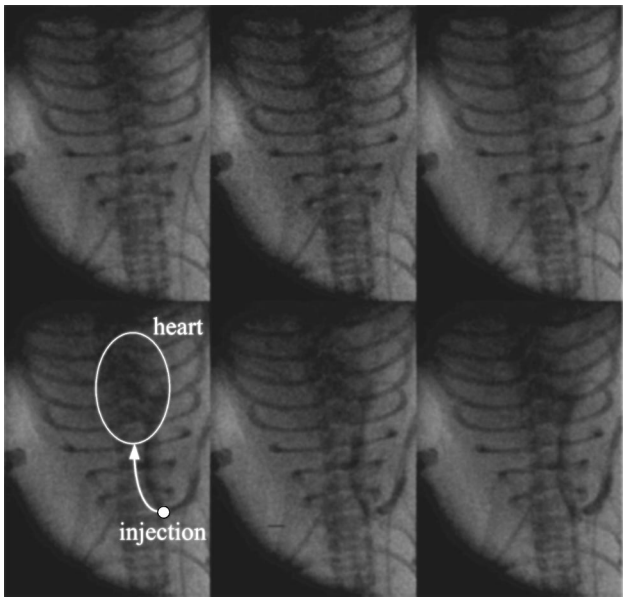

FIG. 6. Gated thoracic imaging of a live rat. The exposure time for each frame is 10 ms. This demonstrates flow of the contrast agent from the injection point to the heart while the lung of the rat remained "still" due to gating.

ration cycle. By viewing the movies rendered from such images, the flow of the contrast media from the injection point to the heart of the rat can clearly be visualized, while the lungs of the rat remain still.

V. DISCUSSION

Here we have demonstrated a simple field emission x-ray source that can generate pulsed x-ray radiation with a temporal resolution as short as 50 ns (limited by the digital pulse generator rather than the source) which is significantly better than state-of-art thermionic x-ray tubes. The current design restricts the tube current to ~ 1 A/cm^2 which, when combined with the sensitivity of the digital detector, puts a limit on the minimum exposure time per frame at about 0.5–1 ms when used for imaging small animals such as rats at ~ 100 μm spatial resolution. The limitation can be overcome in two separate ways. One is to increase the tube current. In a separate study, we demonstrated an emission current density of 30–50 A/cm^2 from a macroscopic cathode.[24] The second is to utilize the gating capability of the system to accumulate data from multiple short exposures to increase the signal to noise ratio as we have demonstrated in this article.

ACKNOWLEDGMENTS

This work was partially supported by the Office of Naval Research and Xintek, Inc. (OZ). We thank Q. Qiu for technical assistance.

[1] A. M. Zolfaghari, E. Kellogg, and S. Wendt *et al.*, Rev. Sci. Instrum. **73**(4), 1945 (2002).
[2] S. V. Tipnis, V. V. Nagarkar, and V. Gaysinskiy *et al.*, IEEE Trans. Nucl. Sci. **49**(5),2415 (2002).
[3] P. Brubacher and B. M. Moores, Radiology **107**(3), 635 (1973).
[4] S. C. Prasad, Med. Phys. **6**(3), 229 (1979).
[5] Robert Gomer, *Field Emission and Field Ionization* (Harvard University Press, Cambridge, MA, 1961).
[6] T. D. Moore, D. Vanderstraeten, and P. M. Forssell, IEEE Trans. Compon., Packag. Manuf. Technol., Part A **25**(2), 224 (2002).
[7] F. M. Charbonnier, J. P. Barbour, and W. P. Dyke, Radiology **117**, 165 (1974).
[8] G. S. Hallenbeck, Radiology **117**, 1 (1974).
[9] Robert Baptist, U.S. Patent No. 6,259,765 (2001).
[10] R. R. Whitlock, M. I. Bell, and D. V. Kerns *et al.*, U.S. Patent 6,333,968 (2001).
[11] M. S. Dresselhaus, G. Dresselhaus, and P. Avouris, in *Topics in Applied Physics*, Vol. 80 (Springer-Verlag, Heidelberg, 2000).
[12] O. Zhou, H. Shimoda, and B. Gao *et al.*, Acc. Chem. Res. **35**, 1045 (2002).
[13] W. A. de Heer, A. Chatelain, and D. Ugarte, Science **270**, 1179 (1995).
[14] A. G. Rinzler, J. H. Hafner, and P. Nikolaev *et al.*, Science **269**, 1550 (1995).
[15] W. Zhu, C. Bower, and O. Zhou *et al.*, Appl. Phys. Lett. **75**(6), 873 (1999).
[16] R. H. Baughman, A. A. Zakhidov, and W. A. de Heer, Science **297**, 787 (2002).
[17] H. Sugie, M. Tanemura, and V. Filip *et al.*, Appl. Phys. Lett. **78**, 2578 (2001).
[18] G. Z. Yue, Q. Qiu, and B. Gao *et al.*, Appl. Phys. Lett. **81**(2), 355 (2002).
[19] O. Zhou and J. P. Lu, U.S. Patent 6,553,096 (2003).
[20] Y. Cheng, J. Zhang, and Y. Z. Lee *et al.*, presented at the International-Symposium-on Clusters and Nano-Assemblies: Physical and Biological Systems, Richmond, 2003 (unpublished).
[21] CEN/TC (European Standard DIN EN 12543-5, 1999).
[22] E. L. Nickoloff, E. Donnelly, and L. Eve *et al.*, Med. Phys. **17**(3), 436 (1990).
[23] B. Ohnesorge and T. Flohr, Electromedica **68**, 1 (2000).
[24] D. Shiffler, O. Zhou, and C. Bower *et al.*, IEEE Trans. Plasma Sci. (to be published).